CLM - P 82

United Kingdom Atomic Energy Authority

RESEARCH GROUP

Preprint

THE DETERMINATION OF ATOMIC COLLISION CROSS SECTIONS USING CROSSED ELECTRON AND ION BEAMS AND SOME SOURCES OF ERROR IN SUCH EXPERIMENTS

M. F. A. HARRISON

Culham Laboratory,

Culham, Abingdon, Berkshire

1965

UNCLASSIFIED
(Approved for publication)

CLM - P82

THE DETERMINATION OF ATOMIC COLLISION CROSS SECTIONS USING CROSSED ELECTRON AND ION BEAMS (AND SOME SOURCES OF ERROR IN SUCH EXPERIMENTS)

by

M.F.A. HARRISON

(Submitted for publication in Brit. J. Appl. Phys.)

A B S T R A C T

Application of the method of crossed beams to the study of collisions between electrons and ions is discussed. Basic principles of the design of a collision region are given and an expression is derived for the collision cross section in terms of the measured electron and ion collision rate. The experimental parameters associated with the derivation are discussed. Simple theories are developed that enable corrections to be made to the measured collision rates to allow for the space charge effects of ion and electron beams. Experimental evidence supporting these theoretical predicitions is given.

U.K.A.E.A. Research Group,
Culham Laboratory,
Nr. Abingdon,
Berks.

July, 1965. (C/18 MEA)

C O N T E N T S

		Page
1.	INTRODUCTION	1
2.	DESIGN OF THE COLLISION REGION AND DETERMINATION OF THE COLLISION CROSS SECTION	2
3.	ERRORS CAUSED BY SPACE CHARGE OF THE BEAMS	7
4.	ACKNOWLEDGEMENTS	16
5.	REFERENCES	17

1. INTRODUCTION

Atomic collision cross sections can be studied by allowing two beams of particlesto collide and measuring the rate at which product particles are formed. This technique is particularly useful if the particles are charged or chemically unstable, and so far has been the only successful method of directly investigating inelastic collisions between electrons and ions. Crossed beams of these particles have been used to study electron impact ionization of ions (for example by Dolder, Harrison and Thonemann, 1961; paper 1) and also electron impact excitation of ions (Dance, Harrison and Smith, 1965; paper 2). The feasibility of a particular investigation depends upon the ability to detect the collision products. Methods of detection applicable to the investigation of various collision processes are shown diagrammatically in Fig.1 and these may be summarised as follows:-

(a) Ions excited to a short lived state can be detected by the photons emitted from the radiative decay of the state whilst the ions are traversing the electron beam.

(b) Ions excited to a metastable state, because of their long lifetime, can be detected some distance beyond the collision region.

(c) Particles resulting from ionization, neutralisation or molecular dissociation can be detected by passing the ion beam through a transverse magnetic field, or alternatively an electrostatic field, thus separating from the parent beam those product particles of different charge or mass.

A disadvantage of the crossed beams technique is that electron and ion densities are so low that many more collisions occur between either beam and residual gas in the apparatus than occur between electrons and ions. Consequently, product ions must usually be observed in the presence of backgrounds arising from extraneous collisions of the beams with residual gas. The electron and ion collision rate can be distinguished from these backgrounds by pulsing the beams and detecting only those product particles whose rate of formation is at the appropriate frequency and phase (Harrison, 1964). The rate of beam pulsing must be faster than any systematic changes in pressure of the residual gas.

Measurement of the electron and ion collision rate is further complicated by the effects of space charge of the beams. Space charge effects can, under certain conditions, change the collision rate. They can also deflect the particle trajectories so that there is a change in the efficiency with which collision products are collected or detected. The latter process can be a major source of error in this type of experiment.

In this paper, the basic principles of the design of the collision region are given and an expression is derived for the collision cross section in terms of the electron and ion collision rate. The experimental parameters associated with this derivation are discussed. In addition, a simple theory is developed that can be used to correct for the effects of space charge upon the collection or detection of collision products. These theoretical predictions are compared with experimental data.

2. DESIGN OF THE COLLISION REGION AND DETERMINATION OF THE COLLISION CROSS SECTION

The collision rate at particular beam currents and energies depends upon the dimensions of the beams and the angle at which they intersect. This rate, and the ratio of its magnitude to backgrounds from collisions between each beam and residual gas, is a maximum if every electron and ion has a chance of colliding. This criterion requires that the beams should be of the same height. Because the ion density is inherently low, $10^{6}\,cm^{-3}$, it is usually necessary to employ large electron beam currents, about $10^{-3}A$, in order to distinguish between the collision rate and the background arising from collisions of the ion beam with residual gas, and also in order to make accurate measurements of small collision rates. At corresponding electron densities, about $10^{7}\,cm^{-3}$, the electron beam expands due to its space charge. Consequently, it is advantageous to make this beam wide, in the direction of ion motion, so that an adequately large beam current can be obtained at low electron densities. This configuration of beams is shown schematically in Fig.2. The shape of the ion beam is defined by an aperture

of height $2h_1$ and width W in the plate P and the electron beam shape by the slit of height $2h_2$ and width ℓ in the anode A of the electron gun. The height of this slit is slightly smaller than the height of the ion beam so that space charge expansion does not cause electrons to pass outside the ion beam. It can be seen later that this expansion can, under certain conditions, produce errors in the measurements. Therefore, the beams are arranged to cross at right angles so that the path length of the electrons is small and the beam spread reduced. In addition, the width W of the ion beam is made small to minimise the distance from the anode to any part of the ion beam.

To determine the collision rate, we assume that mono-energetic ions of a particular species with charge Ne move with a velocity V parallel to the x axis and that mono-energetic electrons with velocity v move parallel to the y axis. The velocity of the electrons relative to the ions is $(V^2 + v^2)^{\frac{1}{2}}$ and the effective length of the electron collision path through the ion beam is

$$C = W (V^2 + v^2)^{\frac{1}{2}}/v . \qquad \ldots (1)$$

The number densities of electrons and ions are usually non-uniform. However, ion motion is in the x direction and so ion density is uniform in this direction. Further, any effects due to variations in ion density in the y direction are averaged out because the electron motion is in this direction. Similar arguments apply to the electron beam and so non-uniformities need be considered only in the z direction.

Electrons passing through an element of height dz and length ℓ located at z encounter an ion density proportional to the ion beam current passing through the element. This current is defined as $i(z)dz$ and so the ion density $\rho(z)$ is

$$\rho(z) = \frac{i(z)}{eNVW} . \qquad \ldots (2)$$

The total flux of electrons passing through this element is $e^{-1}j(z)dz$, where e is the electronic charge and $j(z)dz$ is the electron current. In practice the particle densities in the beams are well within the single collision regime

and so the collision rate in the element dz is

$$K(z)dz = e^{-1}P(z)\, j(z)dz\,, \qquad \ldots (3)$$

where $P(z)$ is the probability that a single electron at height z experiences a collision in passing through the ion beam. It is given by

$$P(z) = Q(\varepsilon)\, \rho(z)\, C\,, \qquad \ldots (4)$$

in which $Q(\varepsilon)$ is the cross section for the particular inelastic collision being studied at an incident electron energy $\varepsilon = m(V^2 + v^2)/2$, where m is the electronic mass.

Substitution for $P(z)$ in equation (3) and integration over the height of the larger beam (in this case the ion beam) yields the total collision rate K, which is given by

$$K = Q(\varepsilon)\, \frac{(V^2 + v^2)^{\frac{1}{2}}}{Ne^2Vv} \int_{-h_1}^{+h_1} i(z)\, j(z)\, dz\,. \qquad \ldots (5)$$

A more convenient form of this equation is

$$Q(\varepsilon) = \frac{2h_1\, Ne^2Vv}{(V^2 + v^2)^{\frac{1}{2}}}\, \frac{K}{IJ}\, F\,, \qquad \ldots (6)$$

where

$$F = \frac{\int_{-h_1}^{+h_1} i(z)dz \int_{-h_1}^{+h_1} j(z)dz}{2h_1 \int_{-h_1}^{+h_1} i(z)\, j(z)\, dz} \qquad \ldots (7)$$

and I and J are respectively the total currents of the ion and electron beams which cross the collision region. In this method, the expression for the cross section (equation 6) is simply that for a uniform larger beam with the factor F included to correct for inhomogeneities in the beams. The factor F, which is dimensionless, is unity if the larger beam is uniform in the z direction, and it may be determined experimentally by the method outlined in paper 1. A shutter, in which is cut an L-shaped slit of height s (see Fig.2), can be lowered to intercept both beams, and the ion beam current $I_s(z)$ passing through the slit

can be measured simultaneously with the corresponding electron beam current $J_s(z)$. The variations of $I_s(z)$ and $J_s(z)$ with z can thus be measured by moving the slit from $z = -h_1$ to $z = +h_1$. If the height of the slit is small, $I_s(z) \approx si(z)$ and $J_s(z) \approx sj(z)$, and so

$$\int_{-h_1}^{+h_1} i(z)dz = I \approx \frac{1}{s} \int_{-h_1}^{+h_1} I_s(z)dz = \frac{A_i}{s} , \qquad \ldots (8)$$

$$\int_{-h_1}^{+h_1} j(z)dz = J \approx \frac{1}{s} \int_{-h_1}^{+h_1} J_s(z)dz = \frac{A_j}{s} , \qquad \ldots (9)$$

and

$$\int_{-h_1}^{+h_1} i(z)j(z)dz \approx \frac{1}{s^2} \int_{-h_1}^{+h_1} I_s(z)J_s(z)dz = \frac{A_{ij}}{s^2} . \qquad \ldots (10)$$

Here, A_i, A_j and A_{ij} are respectively the areas under the curves of $I_s(z)$, $J_s(z)$ and $I_s(z)\,J_s(z)$ plotted against z. Thus

$$F = \frac{A_i A_j}{2h_1 A_{ij}} , \qquad \ldots (11)$$

It should be noted that this expression is independent of s and that any errors incurred due to variation of the beam currents during the measurement of A_i and A_j are likely to be compensated by equal errors in A_{ij}.

In general, the most uncertain parameters in equation (6) are K and F. However, errors in the measurement of F decrease with increasing uniformity of the ion beam, and it has been found using a gaseous ion source and the geometry shown in Fig.2 that F is unlikely to differ by more than 3% from unity. Fig.3 shows typical measurements of $I_s(z)$ and $J_s(z)$ for a $1\mu A$ beam of 5keV He^+ ions and a 1.4 mA beam of 218eV electrons. The measurements were made using an apparatus described in paper 2. This had a collision region defined by $2h_1 = 0.22$cm, $W = 0.1$cm, $2h_2 = 0.16$cm, $\ell = 2.5$cm, $s = 0.012$cm and the distance from the anode A to the ion beam was 0.25cm. The value of F given by these current distributions is 0.99 and so represents a very small correction to the uniform

beams condition despite the non-uniform nature of the electron beam.

The electron current distribution measured by the shutter close to the anode A may differ from the distribution which actually crosses the ion beam because of:

(a) space charge expansion of the electron beam;

(b) the focussing of electron trajectories in the electron gun;

(c) the slight deflection of electron trajectories by the electric field arising from ion space charge.

An additional error can be introduced because the space charge effects of both beams are altered when the shutter is lowered. However, none of these effects cause significant errors if the ion beam is reasonably uniform and if the electron beam is not allowed to become larger in height than the ion beam. The most convenient method of ensuring this latter requirement is to pass the electron beam, which has crossed the ion beam, through a slit whose height is slightly smaller than the ion beam, and to adjust the potentials applied to the electron gun so that negligible electron current is collected at the slit. This arrangement is shown schematically in Fig.8 and in the above apparatus the slit height was 0.18cm. Alternatively, a second shutter can be used to measure the current distribution of the electron beam which has crossed the ion beam. In practice this method has presented difficulties due probably to the space charge of secondary electrons released when the electron beam strikes the shutter in the field free collision region. This difficulty has not been encountered using the shutter close to the anode because secondary electrons are removed by the electric fields in the electron gun.

All errors caused by the previously described effects of space charge are eliminated if the ion beam is uniform and so it can be advantageous to reduce the beam heights so that only the most uniform section of the ion beam passes through the collision region. In addition, it is desirable to make the distance from the anode and shutter to the ion beam, and also the width W of the ion beam, as small as possible.

It may be noted that the collision path is increased if the electron beam is rotated about the axis of the ion beam, and so the collision rate given by equation (5) should be increased by a factor $(\cos \alpha)^{-1}$, where α is the angle of rotation. A correction, for the same reason, is required if the electron beam is either spreading or converging. However, rotation of the electron beam about its own axis affects only the factor F provided that all the electrons pass through the ion beam. If the electron beam does not intersect the ion beam at right angles, both the effective collision path and the relative velocities are changed and so further modification of equation (5) is required. If the electron beam is made larger in height than the ion beam, equation (5) is still valid provided that $-h_2$ and $+h_2$ (where $h_2 > h_1$) are taken as the limits of integration, but errors in the measurement are likely to be larger due to the non-uniform nature of the electron beam. Asymmetries in the dimensions of the beams about the x and y axes can be taken into account by suitable adjustment of the limits of integration.

3. ERRORS CAUSED BY SPACE CHARGE OF THE BEAMS

Space charge slightly changes the energies of the beams due to the potential gradients which exist inside charged beams, but at the densities normally used this effect is negligible. However, the associated electric fields can cause errors due to the deflection of ion trajectories by electron space charge and vice versa. The most significant of these errors are due to:

(a) electron space charge causing losses of ions from the beam by deflection;

(b) electron space charge causing variation of the background arising from the passage of the ion beam;

(c) ion space charge causing variation of the background arising from the passage of the electron beam.

These processes will now be considered in detail.

(a) Losses of ions

In cases where the product ions and parent ions are detected some distance from the collision region, small deflections of the ion trajectories can cause

significant changes in the dimensions of the beams at their collectors. If the undeflected beams are larger than their collectors, then all the ions will not be collected and deflection of the ion trajectories will cause changes in the collected ion currents. Consequently, where this effect differs for the parent and product ion beams, the measured ratio K/I will be in error.

Deflections of the ion trajectories are produced by the electric field arising from the space charge of the electron beam. The electron beam has a height $2h_2$ which is much smaller than its width ℓ so that its associated electric field acts predominantly in the z direction and converges the ion trajectories towards the x axis. There are two consequences of this deflection. Firstly, the current of collected ions increases with increasing electron space charge if the height of the unconverged ion beam is greater than the height of its collector. Secondly, at larger values of electron space charge, the ion trajectories cross the x axis so that the ion beam becomes divergent; consequently, the collected ion current decreases with increasing electron space charge. The y component of electric field due to electron space charge is small and so it is unnecessary to consider ion losses in this direction.

The electric field $U_i(z)$ in the z direction inside an electron beam with a small ratio of height to width and of uniform electron density η is approximately

$$U_i(z) \approx 4\pi\eta ez \qquad (z \leqslant h_2) \; . \qquad \ldots (12)$$

Here, the sign is omitted because it is obvious that the field always converges the ion trajectories. An ion initially moving in the x direction is deflected by this field through an angle $\varphi(z)$ given by

$$\tan \varphi(z) = \frac{\ell U_i(z)}{2T} \; , \qquad \ldots (13)$$

where T is the potential through which the ion has been accelerated before entering the field.

Ions that pass outside the electron beam experience a different field $U_e(z)$

which depends upon the geometries of both the electron beam and the apparatus. At a distance in the z direction from the electron beam small compared to ℓ, it is reasonable to assume that this field is independent of z and that it is given by

$$U_e(z) \approx 4\pi\eta e h_2 \qquad (h_1 \geqslant z > h_2) \quad . \qquad \ldots (14)$$

The deflections produced by the fields expressed by equations (12) and (14) are such that all ion trajectories initially parallel to the x axis that pass through the electron beam are converged in the z direction to a common line focus on the x axis, whereas ion trajectories that lie outside the electron beam are deflected parallel to the envelope of these focussed trajectories.

Fig.4 illustrates the case of initially parallel ion trajectories which are deflected so that they cross the x axis and become divergent. The height $2h_1$ of the ion beam is greater than the height $2h_2$ of the electron beam. Ion trajectories are intercepted at an aperture of height $2h_3$ greater than $2h_1$ located at a distance L from the electron beam, where $L \gg \ell \gg h_3$. The previous arguments indicate that no ions are lost from the beam provided that the electron space charge deflection, φ_2, of the ion trajectory with $z = h_2$, is less than $(h_2 + h_3)/L$. This criterion defines an upper limit of the electron density, which is given by

$$\eta_{max} = \frac{T\,(h_2 + h_3)}{2\pi e h_2 \ell L} \qquad \ldots (15)$$

Typical values are $\eta_{max} \approx 2 \times 10^8$ electrons cm^{-3} for a 5 keV ion beam and a geometry in which $h_2 = 0.1$ cm, $h_3 = 0.5$ cm, $\ell = 3$ cm and $L = 50$ cm. This relationship was investigated in an apparatus that had a similar geometry and which is described in paper 1. The electron current J_{max} that just caused a 5 keV beam of He^+ ions to be intercepted is shown plotted against $E^{\frac{1}{2}}$ in Fig.5, where E is the energy of the electron beam. These results confirm that there is a critical value of electron density, and the measured value of η_{max} agrees within a factor two with that predicted by this very simple theory.

Collision product ions have almost the same velocity as their parent ions

and so, if their mass or charge is different from that of the parent ions, they will be deflected through different angles by the same electron space charge. Consequently the limiting electron density η'_{max} for product ions with mass number M' and charge number N' is

$$\eta'_{max} = \frac{M' N}{M N'} \eta_{max} . \qquad \ldots (16)$$

(b) Variation of the background arising from the ion beam

Losses of parent and product ions can be made negligible by suitable choice of dimensions and ion optics, and also by limiting the electron beam current to a low value. However, a serious complication still remains because of collisions between the ion beam and residual gas in the apparatus. The background arising from this cause may be several orders larger than the collision rate K. Consequently, if the electron space charge can cause the backgrounds to vary, even by a very small fraction, then the variation may well be comparable with K. These variations can only be observed directly at electron energies below the threshold for the electron and ion collision process, and so it is necessary to understand the behaviour of the background at higher electron energies in order to apply a suitable correction to the measured collision rate.

Dolder, Harrison and Thonemann (1963) have discussed the backgrounds encountered in ionization experiments where doubly charged product ions are separated from singly charged parent ions by a magnetic field. In such experiments, the background arises from doubly charged ions formed by charge stripping collisions between parent ions and residual gas. Charge stripped ions are scattered relative to the trajectories of their parent ions and so the product ion beam is divergent. If a significant fraction of this divergent beam is formed before the ions cross the electron beam, and if the divergence is great enough for the ion beam to be larger than its collector, then the background due to charge stripping is increased by the converging action of electron space charge and thus interferes with the measurement of the collision rate.

Excited ions cannot be separated from the parent beam if they have the same

charge. In the excitation experiment described in paper 2, metastable $He^+(2S)$ ions were detected in the presence of a parent beam of $He^+(1S)$ ions that was a factor 10^9 more intense. Consequently, variation of the background arising from the passage of the ion beam through the metastable ion detector (see figure 1) came predominantly from deflections of the parent $He^+(1S)$ ion trajectories by electron space charge.

An accurate analysis of the variation of ion beam background caused by electron beam space charge in experiments such as those cited above is not amenable to a simple but general presentation. The ion beam is usually divergent to an unknown extent due to its own space charge expansion, to poor ion optics, or to scattering collisions with residual gas. The divergence depends upon the geometry of the apparatus, the distribution in the x direction of deflecting fields and scattering atoms both before and after the collision region, and also upon the angular distribution of the scattered ions.

The following approximation, which is illustrated in Fig.6, is sufficiently good for most applications. A rectilinearly divergent ion beam emanates from an element dx located on the axis a distance x before the collision region. The beam passes through the collision region, which is defined by an aperture of height $2h_1$ in the plate P, and then passes through an aperture in the plate P' of height $2h_3$ greater than $2h_1$. The aperture in P' represents the entrance aperture of a collector located at a distance L from the collision region. It is assumed that $h_1 \ll \ell \ll L$. A fraction of the ion beam strikes P' and so the ion current passing through the aperture is increased by the converging action of electron space charge. This is analogous to an increase in ion beam background for a divergent beam that is larger than its detector. The true ion beam is equivalent to a series of such ion beams emanating from elements dx covering a range of values of x. Integration over this range gives the total increase in ion beam current or background. Collimation of the ion beam by the apertures in the plates P and P' defines the maximum value of x which need be considered, because for $x > x_{max}$ all the ion trajectories that pass through the aperture

in P also pass through the aperture in P'. It follows that

$$x_{max} = \frac{h_1}{(h_3 - h_1)} L . \qquad \ldots (17)$$

Scattering collisions produce ions whose trajectories both diverge away from the x axis and converge towards it. The convergent trajectories can be neglected provided the electron space charge is not great enough to cause them to be intercepted at P'.

Ion trajectories emanating from dx and passing through a point at height z in the electron beam lie at an angle $\varphi(z) = zx^{-1}$ relative to the x axis. Since this angle is small, the ion current passing through the element of height dz and length ℓ at z in the electron beam can be defined as $i_d(x,z)dxdz$. At any electron density there exists an ion trajectory, emanating from dx and passing through the electron beam, that is deflected through an angle φ_n such that the ion can just pass through the aperture in the plate P'. The height at which this trajectory passes through the electron beam is h_n and so the angle φ_n is given by

$$\varphi_n = \frac{h_n (1 + Lx^{-1}) - h_3}{L} = \frac{\ell U_n}{2T} , \qquad \ldots (18)$$

where U_n is the electric field due to electron space charge at $z = h_n$. If all the ion trajectories pass through the electron beam,

$$\varphi_n = \frac{2\pi\eta e h_n \ell}{T} . \qquad \ldots (19)$$

This deflection increases the ion current, $I_d(x)dx$, that emanates from dx and passes through P' by an amount, $\Delta I_d(x)dx$, given by

$$\Delta I_d(x)dx = 2 \int_{z=h}^{z=h_n} i_d(x,z)dxdz , \qquad \ldots (20)$$

where

$$h' = \frac{h_3}{(1 + Lx^{-1})} . \qquad \ldots (21)$$

If it is assumed that the ion density is uniform in the z direction, then it

follows from equations (18) to (21) that the fractional increase in the ion current emanating from dx is given by

$$\frac{\Delta I_d(x)}{I_d(x)} = \frac{2\pi\eta eL\ell}{T(1 + Lx^{-1}) - 2\pi\eta eL\ell} . \qquad \ldots (22)$$

The total fractional increase in the ion beam current passing through P', $\Delta I/I$, can be found by integrating $\Delta I_d(x)dx$ and $I_d(x)dx$ between the limits $x = 0$ and $x = x_{max}$. Typical experimental parameters for equation (22) are $T = 5$ kV, $L = 50$ cm, $\ell = 3$ cm, $h_1 = 0.1$ cm, $h_3 = 0.5$ cm, $\eta = 2 \times 10^7$ electrons cm^{-3}, and for these

$$T\,(1 + Lx^{-1}) \geqslant 9\,(2\pi\eta eL\ell) .$$

Thus, for many experimental applications the electron density term in the denominator of equation (22) can be neglected, and so integration with respect to x yields an expression of the form

$$\frac{\Delta I}{I} = \frac{g\eta}{T} = \frac{GJ}{E^{\frac{1}{2}}} , \qquad \ldots (23)$$

where the constants g and G both depend upon the geometry of the apparatus, but G also depends upon the ion beam energy. Equation (23) is exact for ions whose trajectories pass through the aperture in P but lie outside the electron beam.

The measured collision rate K_m includes these contributions from background variations and so can be expressed as,

$$K_m = K + GJI/E^{\frac{1}{2}} . \qquad \ldots (24)$$

It is clear from the geometry shown in Fig.6 that any inclination of the ion beam to the x axis will change the value of x_{max} and so change the constant G. Thus, if K_m is measured at two different inclinations of the ion beam corresponding to G_1 and G_2 and all other parameters remain unchanged, then the difference between these observations can be expressed as

$$\frac{(\Delta I)_1 - (\Delta I)_2}{IJ} = \frac{G_1 - G_2}{E^{\frac{1}{2}}} . \qquad \ldots (25)$$

Measurements of K_m corresponding to $(\Delta I)_1$ and $(\Delta I)_2$ are described in paper 2, and some results are given in Fig.7 which shows $\left[(\Delta I)_1 - (\Delta I)_2\right]/IJ$ plotted against $E^{-\frac{1}{2}}$. Good agreement with equation (25) is demonstrated.

It thus appears probable that backgrounds arising from the passage of an ion beam are in general increased due to the action of electron space charge by a fraction proportional to $E^{-\frac{1}{2}}$. However, the actual magnitude of this increase can only be measured directly at electron energies below the threshold of the particular collision process under investigation.

(c) Variation of the background arising from the electron beam

Backgrounds arising from the passage of the electron beam are likely only in experiments where electrons are detected and in excitation experiments where photons are detected close to the collision region. In the latter type of experiment, backgrounds are caused by photons resulting from electron impact excitation of residual gas and also from bremsstrahlung photons produced when the beam strikes a surface. Photon backgrounds from collisions with gas can be eliminated by beam pulsing techniques (see paper 2), but the background of bremsstrahlung photons can be greatly affected by deflection of the electron trajectories and so is influenced by ion space charge.

Backgrounds due to bremsstrahlung photons were investigated using the apparatus described in paper 2. Photons produced by the electron beam (see Fig.8) were detected by a cylindrical photocathode which was part of a detector for metastable $He^+(2S)$ ions (Harrison, Dance, Dolder and Smith, 1965). The background, B, of photons produced by the electron beam alone was measured as a function of electron energy E and collected current J when the ion beam was turned off. For this particular combination of collision region and photocathode it was given by

$$B = AEJ , \qquad \ldots (26)$$

where A is a constant.

This background was attributed to a small fraction R(E) of the electron beam which struck the plate p located in front of the electron collector, and so

it could also be expressed as

$$B = \lambda(E)\, R(E)\, J , \qquad \ldots (27)$$

where $\lambda(E)$ is the yield of detected bremsstrahlung photons released by incident electrons of energy E.

The background from bremsstrahlung photons was affected when the ion beam was turned on. Considerations similar to those of paragraph 3(b) suggest that, with this particular geometry of electron beam, the fractional increase in electron current passing through the aperture in p due to convergence of electron trajectories by the space charge of an ion beam of current I, can be expressed by

$$\frac{\Delta J}{J} = \frac{HI}{E} . \qquad \ldots (28)$$

Here $-\Delta J$ corresponds to the reduction in electron beam current striking the plate p, and H is a constant depending upon the geometry of the apparatus and the ion beam energy. The corresponding reduction, $-\Delta B$, in the background of bremsstrahlung photons is given by

$$-\Delta B = \lambda(E)\Delta J , \qquad \ldots (29)$$

and so

$$-\frac{\Delta B}{IJ} = \frac{H\lambda(E)}{E} . \qquad \ldots (30)$$

For this particular apparatus equation (30) can be expressed as

$$-\frac{\Delta B}{IJ} = \frac{AH}{R(E)} . \qquad \ldots (31)$$

Thus $-\Delta B/IJ$ varies with electron energy in a manner dictated only by $R(E)$.

It can be seen from Fig.8 that the ion beam passed through the cylindrical photocathode, and so, when the ion beam was turned on, an additional background was observed due to photons produced in collisions between ions and residual gas in the region of the photocathode. The detector was operated so that it was insensitive to photons or metastable ions formed by collisions between ions and electrons, see paper 2, consequently it measured only the combined background, $Y(E)$, of bremsstrahlung photons and photons from collisions of the ion beam with

residual gas. The effects of ion and electron space charge upon this combined background can be expressed by

$$\frac{\Delta Y(E)}{IJ} = \frac{S}{E^{\frac{1}{2}}} - \frac{AH}{R(E)} , \qquad \ldots (32)$$

where S is a constant which defines the effect of electron space charge upon the ion beam background. Measured values of $\Delta Y(E)/IJ$ are shown in Fig.9 by the points plotted against $E^{-\frac{1}{2}}$. It is seen that for energies greater than about 100 eV, the points lie close to the straight line (a). A reasonable interpretation of this observation is that $AH/R(E)$, which is the effect of ion space charge upon electron beam background, is independent of electron energy. This infers that $R(E)$ is also independent of electron energy, which is a reasonable conclusion in view of the design and operating conditions of the electron gun. At energies lower than about 100 eV, the points deviate from the straight line (a). The corresponding decrease of $R(E)$ can be accounted for by the increased electrostatic focussing employed in the electron gun to counteract spreading of the electron beam under the action of its own space charge. The spectral sensitivity of the detector was such that an increase in $\lambda(E)$ was also expected at energies less than about 100 eV, and this is in qualitative agreement with the relationship between $\lambda(E)$ and $R(E)$ shown by equations (26) and (27).

This particular experiment provides some support for the previous arguments, but these do not constitute a generalised theory for the effects of ion beam space charge on background arising from the electron beam. However, in any particular experiment it may be possible to correct in an analogous manner for the ion space charge effect provided the mechanism responsible for the electron background can be identified.

4. ACKNOWLEDGEMENTS

The problems discussed in this paper are based upon evidence obtained in crossed electron and ion beam experiments which were performed at the Atomic Energy Research Establishment, Harwell, and also at the Culham Laboratory,

Abingdon. The author wishes to acknowledge the contributions made to these projects by Dr. K.T. Dolder and by Dr. A.C.H. Smith to whom I am also indebted for much useful advice concerning the present paper. I thank Dr. P.C. Thonemann for his advice and encouragement and also the Director of the Culham Laboratory for his support of these investigations.

5. REFERENCES

DANCE, D.F., HARRISON, M.F.A., and SMITH, A.C.H., 1965, Proc. Roy. Soc. A, in course of publication (referred to as paper 2).

DOLDER, K.T., HARRISON, M.F.A., and THONEMANN, P.C., 1961, Proc. Roy. Soc. A, 264, 367 (referred to as paper 1).

DOLDER, K.T., HARRISON, M.F.A., and THONEMANN, P.C., 1963, Proc. Roy. Soc. A, 274, 546.

HARRISON, M.F.A., 1964, Atomic Collision Processes, edited by M.R.C. McDowell (Amsterdam: North-Holland), p.387.

HARRISON, M.F.A., DANCE, D.F., DOLDER, K.T., and SMITH, A.C.H., 1965, Rev. Sci. Instr., in course of publication.

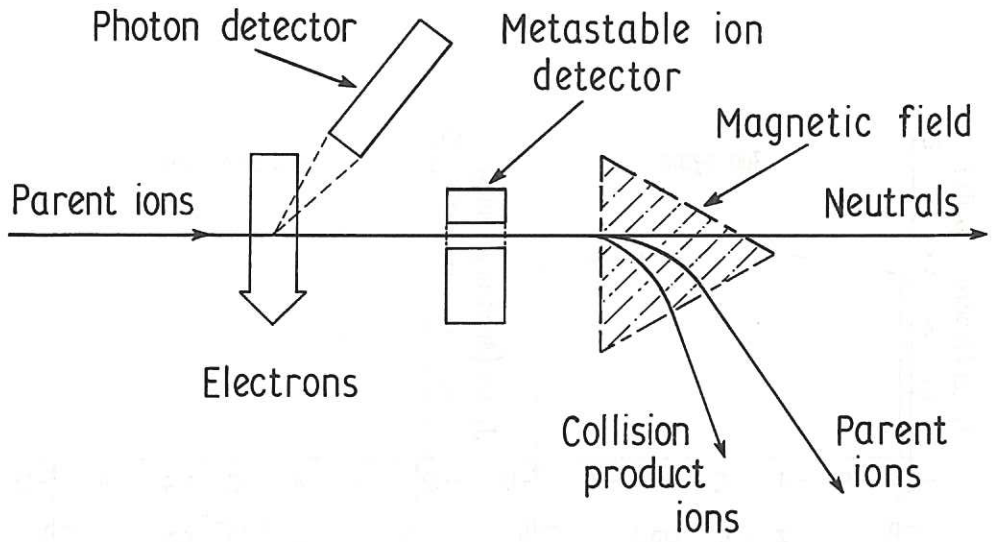

Fig. 1 (CLM-P82)
Detection of collision product particles in crossed electron and ion beam experiments

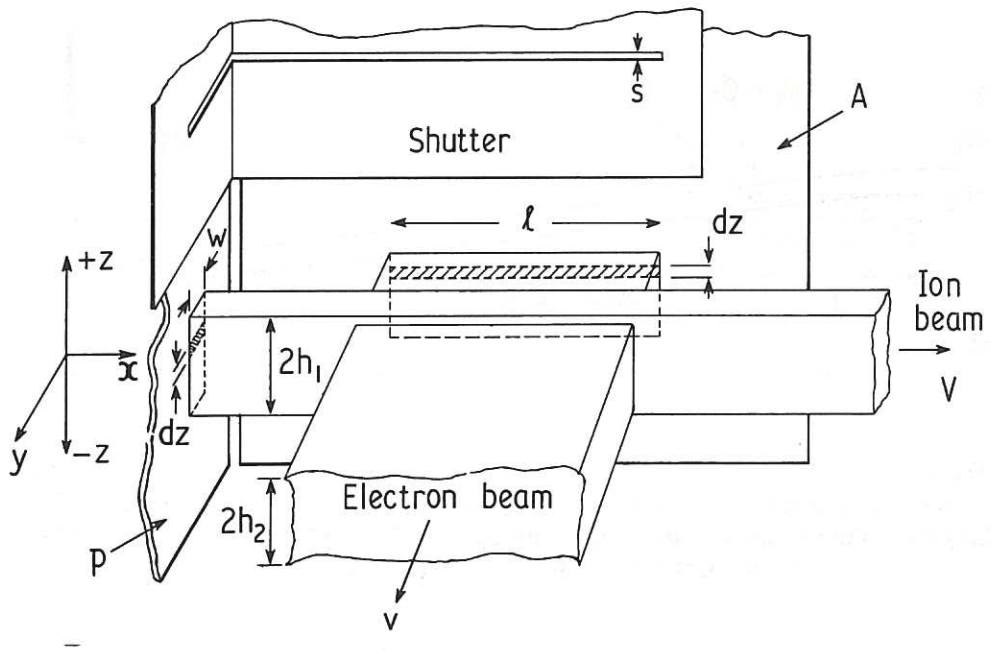

Fig. 2 Schematic diagram of a collision region (CLM-P82)

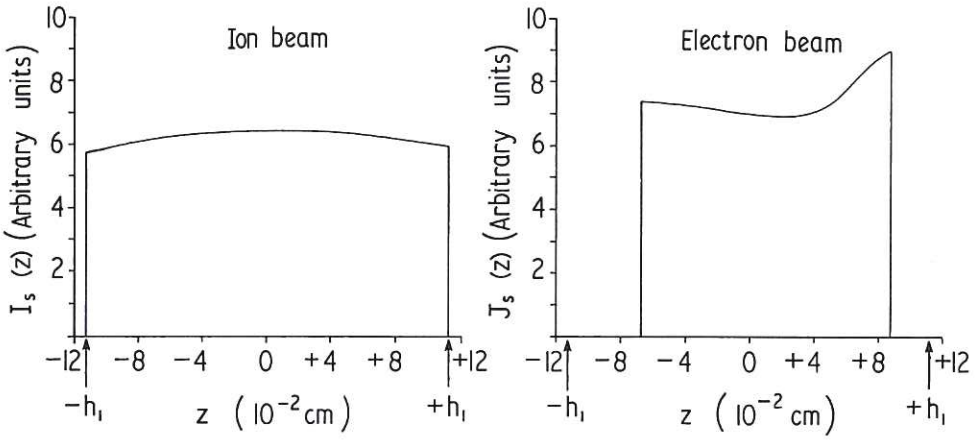

Fig. 3 (CLM-P82)

Typical variation of ion and electron beam current densities in the z direction. Ion beam energy and current were 5 keV and 10^{-6} amp respectively; electron beam energy and current were 218 eV and 1.4 mA respectively

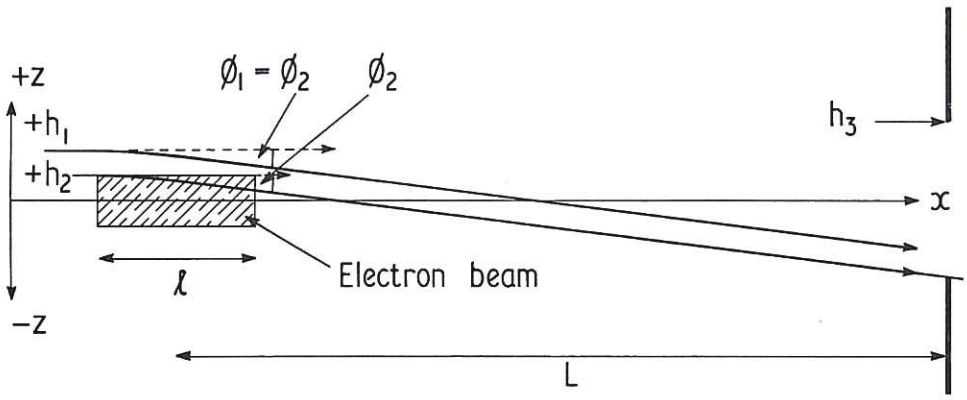

Fig. 4 (CLM-P82)

Converging action of electron space charge on an initially parallel ion beam. The heights of the ion and electron beams are $2h_1$ and $2h_2$ respectively, and the height of the aperture in plate P′ is $2h_3$; $h_3 > h_1 > h_2$

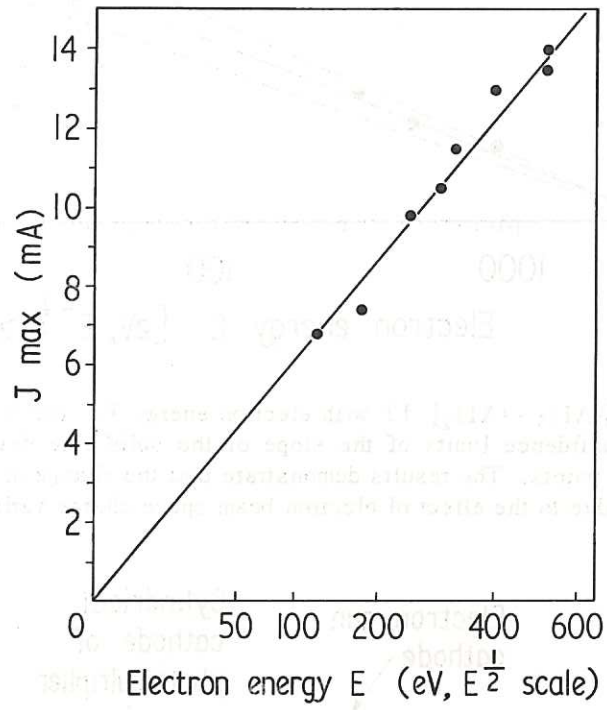

Fig. 5 (CLM-P82)
Critical electron current J_{max} plotted against $E^{1/2}$

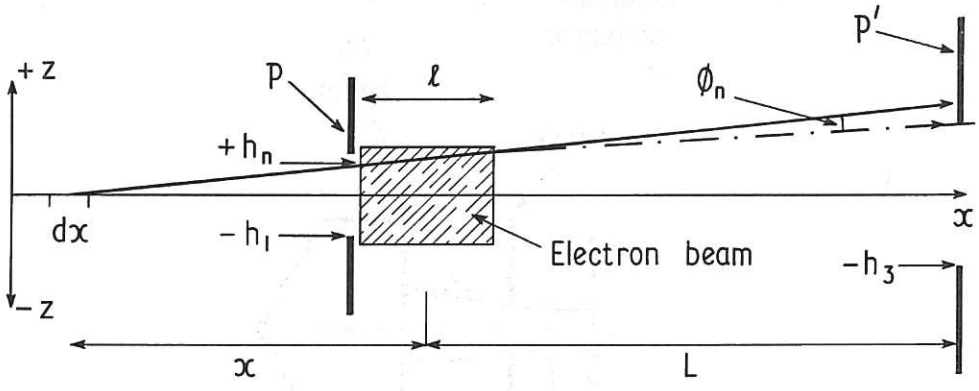

Fig. 6 (CLM-P82)
Converging action of electron space charge upon a diverging ion beam

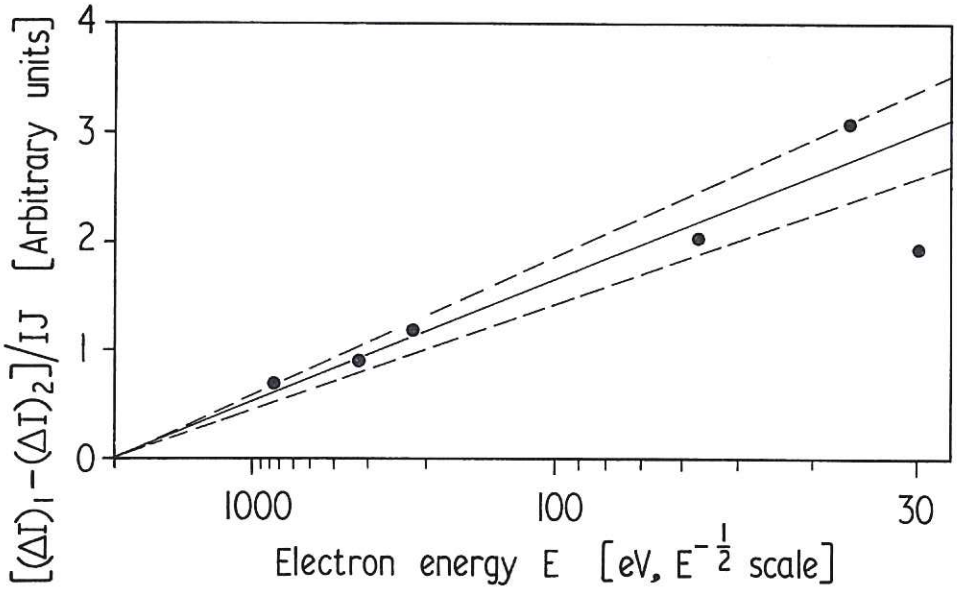

Fig. 7 (CLM-P82)

Variation of $[(\Delta I)_1 - (\Delta I)_2]/IJ$ with electron energy E. The broken lines indicate 90% confidence limits of the slope of the solid line drawn through the experimental points. The results demonstrate that the change of ion beam background due to the effect of electron beam space charge varies as $E^{-\frac{1}{2}}$

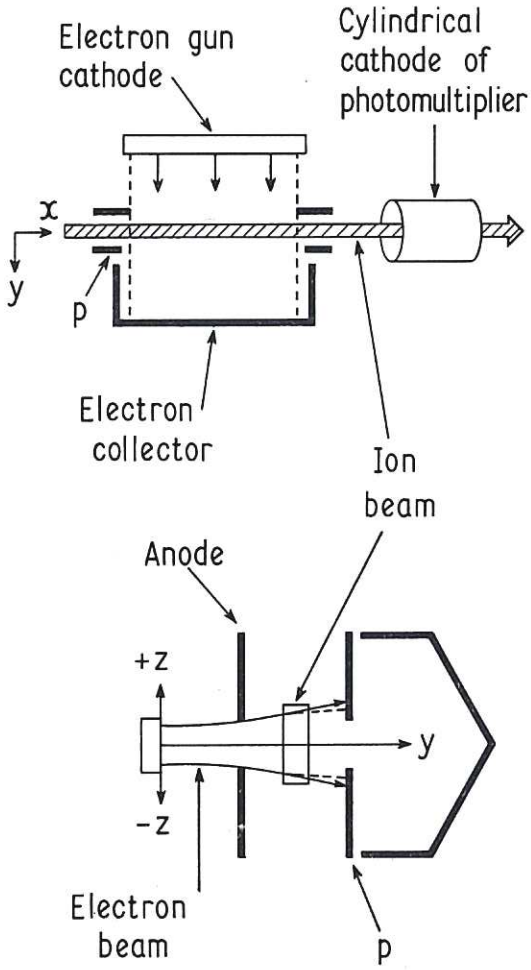

Fig. 8 (CLM-P82)

Apparatus used to investigate backgrounds from bremsstrahlung photons; upper diagram, plan view; lower diagram, section through the electron beam viewed in the direction of the ion beam

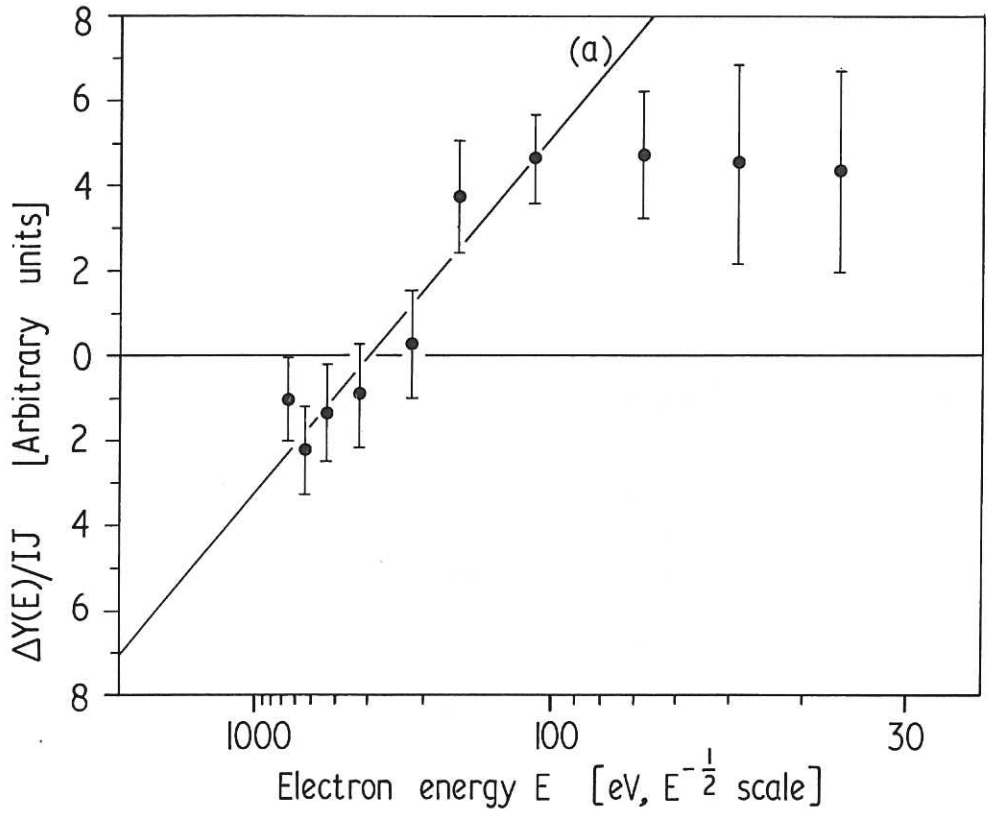

Fig. 9 (CLM-P 82)

Variation with electron energy E of the change $\Delta Y(E)$ of combined ion and electron background due to ion and electron beam space charge. The brackets represent 90% confidence limits